

Response Analysis of Base Isolated Structure with Nonlinear Damper

Akira SONE, Shizuo YAMAMOTO
Kyoto Institute of Technology, Kyoto, Japan

1 INTRODUCTION

For a decade, seismic base isolation systems utilizing the laminated rubber bearings have been studied and they have been applied to various structures such as buildings (Lee and Medland 1979; Kuroda et al. 1989). Recently, these systems have been investigated to advance the feasibility of FBR(Fast Breeder Reactors)(Shojiri et al. 1989). Generally, these systems shift the fundamental natural period of the isolated structure away from the range of dominant period of the horizontal seismic ground motions, such that the seismic response transmitted to the structure will be reduced.

However, some long-period ground motions having the large displacement, including the period range between 1 and 15 second, such as the Great Kwanto Earthquake were recorded(Morioka 1980). According to the resonance phenomenon with long-period ground motion, the displacement response of the base isolated structure becomes quite large. Therefore, base isolation systems incorporate various types of energy absorbing devices such as viscous damper, elasto-plastic damper and so on.

In this paper, to suppress such the large displacement response of the base isolated structure, two types of nonlinear damper are studied and applicability of these nonlinear dampers are examined analytically. These nonlinear dampers have the advantage such that they operate weakly in the range of small displacement and operate strongly against the large displacement.

2 ANALYTICAL MODEL AND DAMPING PROPERTY ON NONLINEAR DAMPER

First, to simulate the seismic response of the base isolated structures with nonlinear damper, a single degree of freedom model is used as shown in Fig. 1. The equation of motion of this model is expressed as follows.

$$m\ddot{x} + kx + f(x, \dot{x}) = -m\ddot{y} \quad (1)$$

where m and k are the mass of isolated structure and the spring constant of rubber bearing, respectively. Also, x and y are the relative displacement response and seismic inputted ground motion, respectively. The damping force $f(x, \dot{x})$ due to the nonlinear damper as shown in Fig. 2 is proposed in this study. This damping force is expressed as the following equation (Yamamoto and Takakura 1988; Yamamoto 1989).

$$f(x, \dot{x}) = \begin{cases} cx^i \dot{x}^j & ; x>0, \dot{x}>0 \\ -cx^i \dot{x}^j & ; x<0, \dot{x}<0 \\ 0 & ; x \cdot \dot{x} \leq 0 \end{cases} \quad (2)$$

In this equation, i and j express the power i th and j th of the relative displacement and relative velocity, respectively. From a practical standpoint, in this study, two types of nonlinear dampers given by Eq.(2) with $i=j=1$ and $i=j=2$ are studied. Here, these nonlinear are abbreviated to " $x^1 \dot{x}^1$ " and " $x^2 \dot{x}^2$ ". Also, c in Eq.(2) is a coefficient which gives the shape of damping force of nonlinear damper. In Fig. 2, x_p is maximum displacement of nonlinear damper. These dampers have the advantage such that they operate weakly in range of small displacement and operate strongly against the large displacement. The absorbing energy per a cycle of sinusoidal wave due to these dampers corresponds to the area of hysteresis loop and is given by

$$W_d = \frac{\Gamma(i+1/2) \Gamma(j+2/2)}{\Gamma(i+j+3)} c \omega^j x_p^{i+j+1} \quad (3)$$

where (\cdot) is the gamma function. By applying the averaging method(Minorsky 1962) to the fundamental harmonic component expanded into Fourier series for the damping force, the equivalently linearized damping coefficient c_{eq} and spring constant k_{eq} are given by

$$c_{eq} = \frac{\Gamma(i+1/2) \Gamma(j+2/2)}{\pi \Gamma(i+j+3/2)} c \omega^{j-1} x_p^{i+j-1} \quad (4)$$

$$k_{eq} = \frac{\Gamma(i+2/2) \Gamma(j+1/2)}{\pi \Gamma(i+j+3/2)} c \omega^j x_p^{i+j-1} + k \quad (5)$$

where ω is a angular frequency of input motion. For two types of nonlinear dampers, calculated W_d by Eq.(3) and calculated equivalent damping ratio ζ_{eq} by using c_{eq} and k_{eq} of Eqs.(4) and (5) are shown in Figs. 3 and 4. These figures are obtained by taking a natural angular frequency of isolated structure $\omega_0 = \sqrt{k/m} = \pi$ (rad/s) and an angular frequency of exciting force $\omega = \pi$ (rad/s), and by equivalizing the absorbing energy W_d of two types of dampers at $x_p = 20$ cm. Here, W_d and ζ_{eq} are nondimensional values by those of $x^2 \dot{x}^2$ -type damper at $x_p = 20$ cm. Also, r on abscissa is normalized by $x_p = 20$ cm. From these figures, it becomes clear that W_d and ζ_{eq} of both dampers become large as x_p increases.

3 RESPONSE PROPERTIES OF ISOLATED STRUCTURE WITH NONLINEAR DAMPER

First, the steady state response of isolated structure subjected to a sinusoidal motion $y = y_0 \sin \omega t$ is considered. The transmissibility τ_1 of relative displacement response and transmissibility τ_2 of absolute acceleration response of model in Fig. 1 are calculated by using c_{eq} and k_{eq} of Eqs.(4) and (5). The calculated results are shown in Figs. 5 and 6. Figures 5 and 6 are for the isolated structures with $x^1 \dot{x}^1$ -type damper and $x^2 \dot{x}^2$ -type damper, respectively. In these figures, the dashed curve and solid curve correspond τ_2 and τ_1 , taking two values as a parameter c/m . Also, λ on abscissa is a frequency ratio ω/ω_0 . From these figures, it can be shown that both nonlinear dampers reduce the peak values of two transmissibilities τ_1, τ_2 as c/m increases, namely the nonlinearity of dampers becomes large. Also, in the range of large frequency ratio λ , the value of the transmissibility becomes small. Therefore, two types of nonlinear dampers

can suppress the large displacement response of base isolated structure subjected to ground motion having long period component and are effective as a isolation device for the ground motion with relatively short period.

From above transmissibilities, the amplification factor x_{\max}/y_0 of relative displacement response and that of $\ddot{z}_{\max}/y_0\omega^2$ of absolute acceleration response under the resonance condition of $\omega = \omega_0$ are given as follows.

(1) In the case of $x^1\dot{x}^1$ -type damper

$$x_{\max}/y_0 = (3\sqrt{2} \omega_0^2 m / 4\pi c y_0)^{1/2} \quad (6)$$

$$\ddot{z}_{\max}/y_0\omega^2 = (1 + 3\pi\omega_0 m / 2c x_{\max} + 9\pi^2\omega_0^2 m / 8c^2 x_{\max}^2)^{1/2} \quad (7)$$

(2) In the case of $x^2\dot{x}^2$ -type damper

$$x_{\max}/y_0 = (15\sqrt{2} \pi m / 8c y_0^3)^{1/4} \quad (8)$$

$$\ddot{z}_{\max}/y_0\omega^2 = (1 + 15\pi m / 4c x_{\max} + 225\pi^2 m^2 / 32c^2 x_{\max}^6)^{1/2} \quad (9)$$

Taking the values from 1 to 30 cm as a parameter of y_0 for a constant values of c/m , the amplification factors x_{\max}/y_0 and $\ddot{z}_{\max}/y_0\omega^2$ calculated by above equations are shown in Figs. 7 and 8. Figure 7 shows the calculated x_{\max}/y_0 of Eqs.(6) and (8), and Fig. 8 shows the calculated $\ddot{z}_{\max}/y_0\omega^2$ of Eqs.(7) and (9). In these figures, ζ_{eq} on abscissa is used in order to compare the results obtained from two types of dampers. Also, the symbols \circ and \bullet correspond the simulation results obtained from $x^1\dot{x}^1$ -type damper and $x^2\dot{x}^2$ -type damper. From these figures, it is clear that both x_{\max}/y_0 and $\ddot{z}_{\max}/y_0\omega^2$ calculated from $x^1\dot{x}^1$ -type damper are almost equal to those calculated from $x^2\dot{x}^2$ -type damper. In the case of x_{\max}/y_0 in Fig. 7, the calculated results agree well with the simulation for both dampers, irrespective of ζ_{eq} . This means relative displacement response of isolated structure is dominated and affected by the fundamental harmonic component.

On the other hand, in the case of $\ddot{z}_{\max}/y_0\omega^2$ in Fig. 8, the calculated results agree with the simulation results in range of small ζ_{eq} . However, their difference becomes large as ζ_{eq} increases. Therefore, the acceleration response seems to be affected by the higher harmonic component as the damping force of damper becomes large. Also, by comparison of the simulation results for two types of dampers, the effect of higher harmonic component for $x^1\dot{x}^1$ -type damper is smaller than that for $x^2\dot{x}^2$ -type damper. In order to investigate this effect, the response time histories of isolated structures with $x^1\dot{x}^1$ -type damper and $x^2\dot{x}^2$ -type damper are shown in Fig. 9 for $\zeta_{eq}=0.25$ for both dampers. In this figure, dashed wave form and solid wave form correspond to the results obtained from $x^2\dot{x}^2$ -type and $x^1\dot{x}^1$ -type dampers, respectively. In this figure, the maximum relative displacement response for $x^1\dot{x}^1$ -type damper becomes equal to that for $x^2\dot{x}^2$ -type damper. However, the maximum acceleration responses for these dampers do not agree because of their spikes in their wave forms, that is the effect of higher harmonic component. Accordingly, it is also clear that the maximum acceleration response for $x^1\dot{x}^1$ -type damper is smaller than that for $x^2\dot{x}^2$ -type damper.

Next, under the above same condition concerning $\zeta_{eq}=0.25$, the comparison of response time histories of isolated structures with two types of dampers subjected to the real earthquake motion, El Centro NS(maximum input acceleration = 3.417 m/s²), is shown in Fig. 10. This figure shows that both nonlinear dampers can have the isolating effect from the ground acceleration with relatively short period. And, from the comparison between two type dampers, it is clear that both maximum displacement and acceleration responses for $x^1\dot{x}^1$ -type damper is smaller than those of $x^2\dot{x}^2$ -type damper.

4 CONCLUSIONS

In order to suppress the large displacement response of base isolated structure, two types of nonlinear dampers are studied by the analytical method and numerical simulations.

The results obtained herein are summarized as follows.

- (1) From the transmissibility for isolated structures with these nonlinear dampers, it is shown that the proposed nonlinear dampers can effectively reduce the displacement responses transmitted to the isolated structures against the seismic ground motions having both long and short periods.
- (2) From the comparison between the results obtained by two types nonlinear dampers, it is shown that $x^1\dot{x}^1$ -type damper becomes more resonable than $x^2\dot{x}^2$ -type damper in order to reduce the acceleration response of isolated structure.

5 REFERENCES

- Kuroda, et al.(1989). Verification Studies on Base Isolation Systems by Full-Scale Building, Proc. 1989 ASME PV&P Conf., PVP-Vol.181, pp.1-8.
 Lee, D. M. and Medland, I. C.(1979). Base Isolation systems for Earthquake Protection of Multi-story Shear Structure. Earthquake Engineering Structurala Dynamics. Vol. 7, pp.555-568.
 Minorsky, N. (1962). Nonlinear Oscillations, Van Nostrand Co.
 Morioka, T. (1980). The Great Motion of the Great KANTO Earthquake of 1923. Trans. of Architectural Institute of Japan, No.289, pg79-91.
 Shiojiri, H. et al. (1989). Seismic Isolation for FBR-Preliminaryt Study, Proc. 1989 ASME PV&P Conf. PVP-Vol.181, pp115-120.
 Yamamoto, S. and Takakura, N.(1988). Research on Nonlinear damper Installed to the Isolated Structure, Proc. 1988 ASME PV&P Conf. PVP-Vol.147, pp.45-47.
 Yamamoto, S. et al.(1989). Development of Non-linear Damper Installed to the Base Isolated Structure, Proc. 1989 ASME PV&P Conf., PVP-Vol.181, pp.73-78.

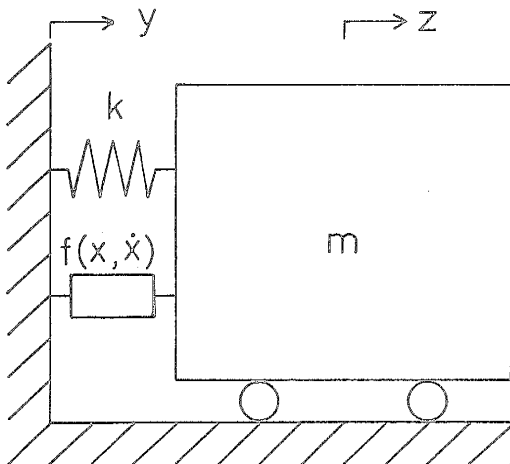


Fig. 1 Analytical model of base isolated structure

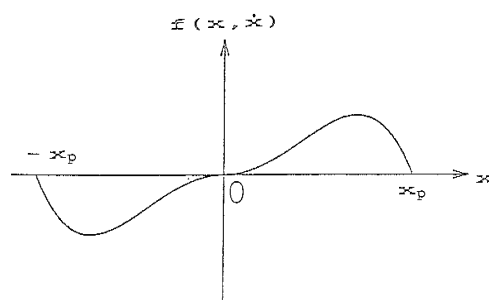


Fig.2 Damping force of nonlinear damper

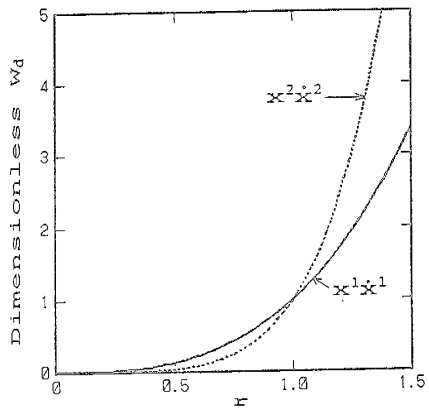


Fig. 3 Comparison of absorbing energy

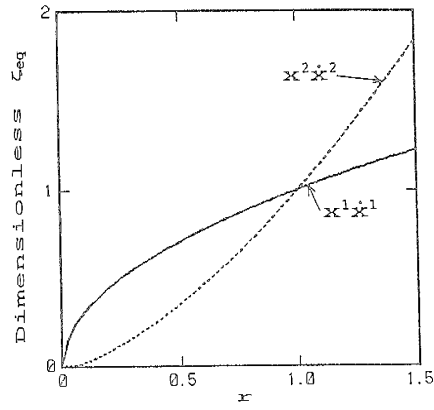


Fig. 4 Comparison of equivalent damping ratio

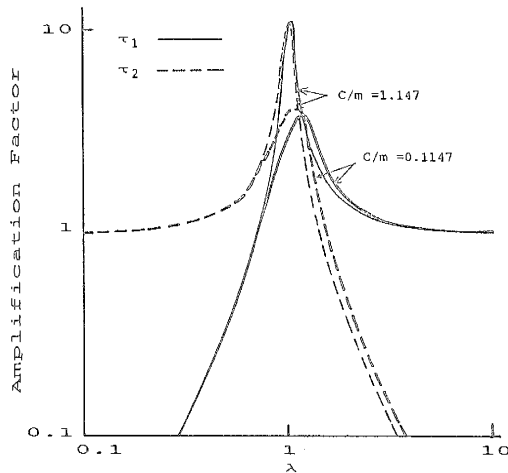


Fig. 5 Transmissibility of isolated structure with $x^1 \dot{x}^1$ -type damper

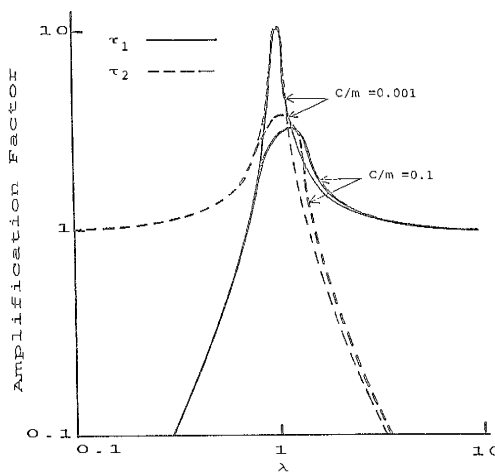


Fig. 6 Transmissibility of isolated structure with $x^2 \dot{x}^2$ -type damper

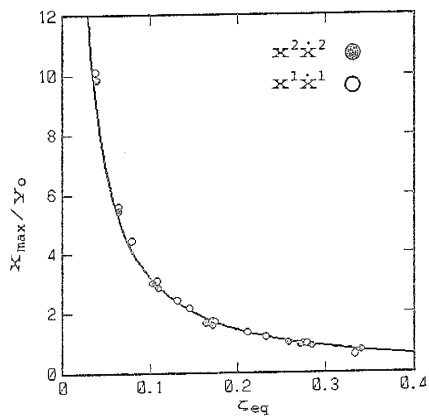


Fig. 7 Relation of x_{max}/y_0 and ζ_{eq}

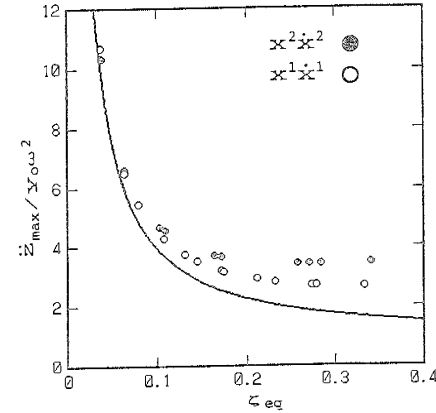
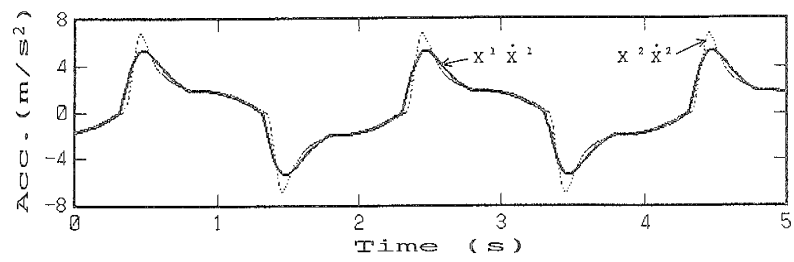
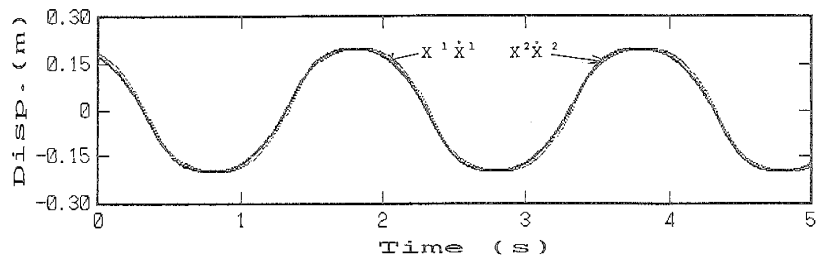


Fig. 8 Relation of $z_{max}/y_0\omega^2$ and ζ_{eq}

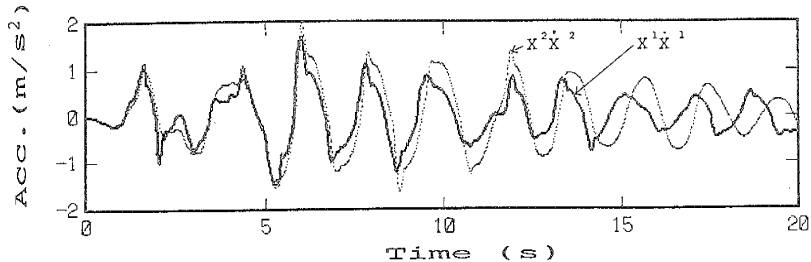


(a) Absolute acceleration response

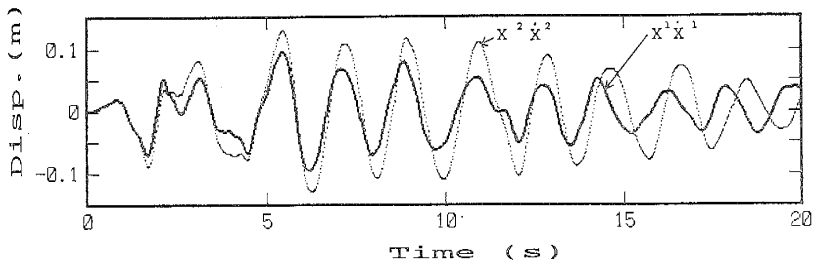


(b) Relative displacement response

Fig. 9 Comparison of response time histories(Sinusoidal motion)



(a) Absolute acceleration response



(b) Relative displacement response

Fig. 10 Comarison of response time histories (El Centro NS)